Electronic Supplementary Material (ESI) for Journal of Materials Chemistry A.

Supplementary Information

Lithium Insertion in Hard Carbon as Observed by ^{7}Li NMR and XRD. Local and Mesoscopic Order and Their Relevance for Lithium Storage and Diffusion

*Yuan Fang, Kevin Peuvot, Alice Gratrex, Evgeny V. Morozov, Johan Hagberg, Göran Lindbergh and István Furó**

Additional sample details

Table S1. The potentials, reversible or total specific capacity and the reversible or total stoichiometry of Li for the four different samples (see Figure 1) investigated. Note that the first cycle loss is taken into account for the total Li stoichiometry and total specific capacity as it will contribute to ^{7}Li NMR signal.

Voltage [V]	Reversible specific capacity [mAh/g]	Lithium reversible stoichiometry	Total specific capacity [mAh/g]	Lithium total stoichiometry
0.003	307	$LiC_{7.3}$	384	$LiC_{5.8}$
0.150	197	$LiC_{11.3}$	274	$LiC_{8.1}$
0.300	103	$LiC_{21.7}$	180	$LiC_{12.4}$
0.500	52	$LiC_{42.9}$	129	$LiC_{17.3}$
0.9	36	$LiC_{62.0}$	106	$LiC_{21.1}$
2	0	N/A	77	LiC_{29}

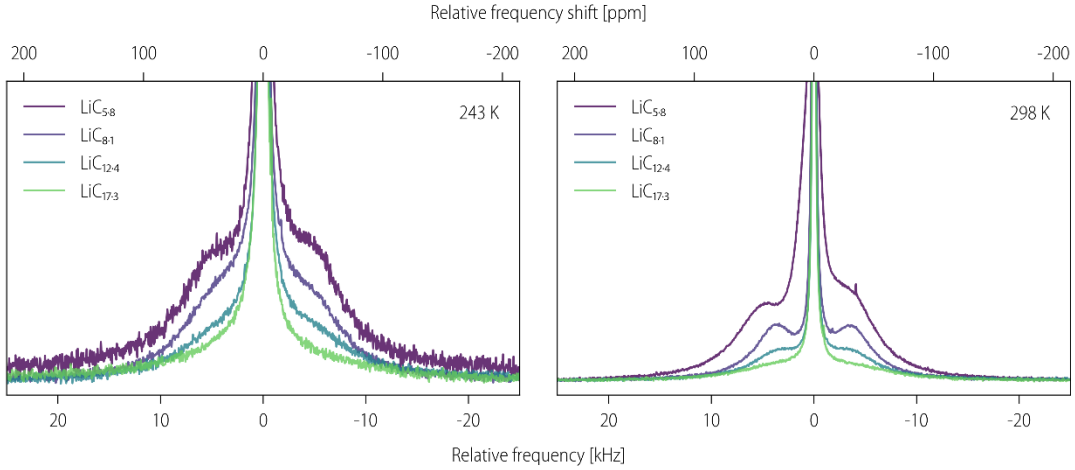

Fig. S1 Comparison of line shapes of lithiated PAN fibers of different lithium content at 243 K and 298 K.

The thermal stability of the samples was tested by recording the NMR spectra of the samples at different temperatures. The fully lithiated sample showed itself to be the least chemically stable and the changes in its ^{7}Li frequency shift at different temperatures and over different time periods is shown below in Table S2.

Table S2. The frequency shift change of the ^{7}Li NMR signal with time at different temperatures for the fully lithiated CF at capacity of 384 mAh/g.

	Frequency shift change (ppm)			
Time (h)	333 K	343 K	353 K	363 K
0	0	0	0	0
4	0.25	0.43	0.59	2
8	0.34	0.60	0.76	2
12	0.44	0.67	0.87	3
16	0.49	0.73	0.93	3
24	0.56	0.85	1.04	3

Table S3. The diffusion coefficients measured parallel and perpendicular to the fiber direction for CFs at different lithium content.

	$D_{parallel}$ (10^{-12} m^2/s)	$D_{perpendicular}$ (10^{-12} m^2/s)
$LiC_{5.8}$	14.4 ± 1.7	1.49 (+1.64/-1.49)
$LiC_{8.1}$	5.25 ± 0.6	0.91 ± 0.17
$LiC_{12.4}$	1.73 ± 0.07	0.13 ± 0.13
$LiC_{17.3}$	0.59 ± 0.06	1.14 ± 0.29

Table S4. Estimated T_1 (from inversion recovery) and T_2 (from spin echo) values measured at 343 K at 194.4 MHz. The T_1 values obtained at different temperatures are displayed in Fig. 4.

Sample	T_1[a] (s)	T_1[b] (s)	T_2[a] (ms)	T_2[b] (ms)
$LiC_{5.8}$	0.144	0.156	0.65[c]	0.3
$LiC_{8.1}$	0.203	0.55	1.7	0.7
$LiC_{12.4}$	0.215	0.208	1.6	1.2
$LiC_{17.3}$	0.232	0.192	1.3	0.9

a. CFs parallel to the magnetic field.
b. CFs perpendicular to the magnetic field.
c. At 298 K, the estimated T_2 is 0.1 ms.

Skin depth calculation

The skin depth at ^{7}Li NMR frequencies was calculated according to the equation: $d = \sqrt{\frac{1}{\pi f \sigma \mu_0 \mu_r}}$ where f is the NMR frequency (either 116.64 MHz or 194.37 MHz), σ the conductivity of the tested carbon fiber, μ_r the relative magnetic permittivity taken as $\mu_r = 1$ and μ_0 the vacuum permeability 1.257×10^{-6} H/m. With conductivity data available[1] as $\sigma = 7.7 \times 10^4$ S m^{-1} the skin depth is estimated to 142 μm at 116.64 MHz and 110.0 μm at 194.37 MHz that is far below the 5 μm diameter of individual fibers.

XRD data treatment

In order to extract the structure factor $S(q)$ one must rely on some corrections[2]. Electron recoil from a scattering atom produces inelastic Compton scattering $S(x, Z)$, where $x = q/4\pi$, which equals zero at $x = 0$ and rises to a constant value at a rate and level that depends on the atom involved, for which analytical approximations exist[3].

Scattering events with x-rays are electromagnetic interactions, and as such are photon-electron interactions; the atomic nucleus is largely irrelevant. As the wavelength of x-rays (in the order of 1Å) are similar to the dimensions of the diffuse electron cloud, this leads to two additional contributions to the observed scattering signal. Firstly, there is the atomic form factor $F(x, Z)$, which describes the interaction between an incoming wave and the electron cloud of an isolated atom. $F(x, Z)$ is typically interpolated between calculated theoretical values[4], for which we used the Akima algorithm[5]. Similarly, the structure factor requires 'de-broadening' to remove the contributions from the electron cloud. The broadening function we used was the product of the density of the carbon fibres (1.78g/cm^3) and the square of the form factor[2].

Early work by Franklin showed that failing to perform these corrections led to overestimations of the interlayer spacing in disordered carbons[6]. To do so, it is necessary to place the scattering intensities on an absolute scale in electron units. There are rigorous methods of doing this (see, for example, in reference [7] and [8]), but a reasonable approximation can be achieved by scaling the observed scattering intensity until it matches the sum of the calculated Compton scattering and self-scattering contributions, which can then be subtracted.

The method for retrieving the structure factor $S(q)$ from the observed intensities $I(q)$ is thus

$$S(q) = \frac{I(q) - (S(x, Z) + F(x, Z)^2)}{1.78 \times F(x, Z)^2 \times e^{-\sin\theta}}$$

The anisotropy of average diffusion coefficient

As discussed in the main text, in our structural model for mesoscopic order we explore graphitic domains with their *c* axis perpendicular to the fiber axis and isotropically distributed within the plane perpendicular to the fiber axis. We also assume that lithium species diffusing sample many such domains. Hence, we measure an average diffusion coefficient in either directions. The effect reaches it maximum if, within the graphitic domains, the diffusion along the *c* axis that is, perpendicular to the graphitic planes is zero, while perpendicular to the *c* axis that is

parallel to the graphitic planes is a finite value D_0. In such a case, diffusion *along* the fiber axis proceeds in all domains by the same diffusional coefficient, that is D_0. On the other hand, diffusion *perpendicular to* the fiber axis proceeds in a domain oriented by its *c* axis at angle θ wrt the applied magnetic field gradient by the effective diffusion coefficient $D_0 \cdot \sin\theta$ that characterizes displacement along the gradient direction. If is distributed isotropically in the plane perpendicular to the fiber axis, the ratio of the average diffusion coefficients *perpendicular and parallel to* the fiber axis becomes $\frac{\langle D \rangle_{\perp}}{\langle D \rangle_{\parallel}} = \frac{\int_0^{\pi/2} D_0 \cos\theta \, d\theta}{\int_0^{\pi/2} D_0 \, d\theta} = \frac{2}{\pi}$.

Illustrative diffusional decay data

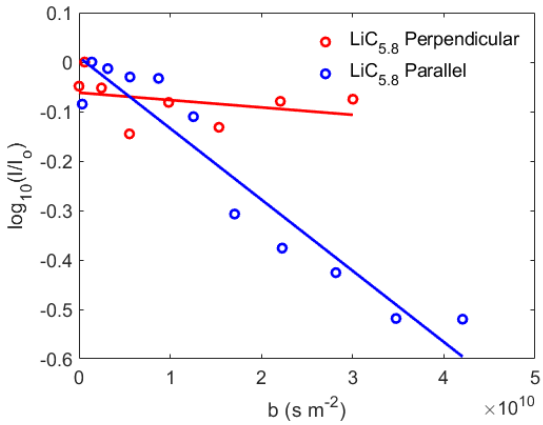

Figure S2. The diffusional decay of ^{7}Li signal from the fully lithiated sample $LiC_{5.8}$ at 343 K when sample was placed parallel (blue) to and perpendicular (red) to the magnetic field. Parameter *b* is $\gamma^2 g^2 \delta^2 (\Delta - \delta/3)$ where γ is the magnetogyric ratio of ^{7}Li while the other parameters are provided in the main text.

References

1. M. H. Kjell, T. G. Zavalis, M. Behm and G. Lindbergh, *J. Electrochem. Soc.*, 2013, **160**, A1473-A1481.
2. A. K. Soper and E. R. Barney, *J. Appl. Cryst.* , 2011, **44**, 714-726.
3. H. H. M. Balyuzi, *Acta Cryst.*, 1975, **A31**, 600-602.
4. J. H. Hubbell, W. J. Veigele, E. A. Briggs, R. T. Brown, D. T. Cromer and R. J. Howerton, *J. Phys. Chem. Ref. Data*, 1975, **4**, 471-538.
5. H. Akima, *J. ACM*, 1970, **17**, 589–602.
6. R. E. Franklin, *Acta Crystallogr.*, 1950, **3**, 107-121.
7. J. Krogh-Moe, *Acta Cryst.*, 1956, **9**, 951-953.
8. N. Norman, *Acta Cryst.*, 1957, **10**, 370-373.